Reducing Interference in Human–Robot Collaboration: A Distance-Based Policy for Disassembly Collaborative Task

Wendy Cahya Kurniawan, Wen Liang Yeoh, Osamu Fukuda
Department of Computer Science and Intelligent Systems, Saga University, Japan

***Abstract*—This study investigates human-robot collaborative (HRC) disassembly tasks, focusing on the effects of constrained and unconstrained safety distances on human behavior and movement interference. Separate and shared target configurations were compared using a screw-picking task as a prototype for electronic waste (e-waste) disassembly. The system employ a vision-based approach to track screws, the human hand, and the robot end effector. Performance was evaluated using objective metrics, including completion time, warning distance, and movement heatmaps, as well as subjective workload assessed via NASA-TLX. Results show that the safety algorithm significantly improved movement efficiency by minimizing the spatial distribution compared to the unconstrained trials. Furthermore, significant results from the factorial design showed that separate-target task enhanced human awareness, enabling participants to anticipate warning distances more effectively than the shared-target task. Synchronizing task assignments with safety algorithms reduces the need for human intervention.**

***Keywords*—Human-robot collaboration; disassembly collaborative task; UI feedback; distance policy; vision-based sensor**

I. Introduction

Although the Industrial Revolution enabled significant technological advancements, it also introduced substantial challenges. Industry 4.0, integrating automation, big data, the Internet of Things (IoT), and artificial intelligence (AI), enhances productivity and efficiency [1], [2]. However, these advancements have caused a rapid increase in electronic waste (e-waste), posing a significant threat to environmental sustainability [3], [4]. Effective global waste management is essential for sustainability, with disassembly playing a critical role in material recovery [5]–[7]. However, disassembly is significantly more challenging to automate than assembly owing to the variability in product types. The disassembly process requires a high degree of flexibility to manage technical and economic uncertainties, which is crucial for enabling widespread industrial adoption.

The Industry 5.0 paradigm addresses these productivity and flexibility challenges [8]. Leveraging advancements in lightweight robots, human-robot collaboration (HRC) workspace can enhance efficiency and productivity, while prioritizing human safety in shared environments. Several studies have aimed to accelerate disassembly tasks, including disassembly sequence planning (DSP). Task assignment algorithms, such as the Discrete Bees Algorithm [9] and Genetic Algorithm [10], have been developed to optimize human–robot labor division under specific safety constraints [11], [12].

From a human-centered system perspective, experimental studies examining real-time human movement during collaborative disassembly task allocation are lacking. Additionally, the impact of task type—whether spatially separated or shared—on human safety, efficiency, and workload has not yet been systematically investigated. Although objective safety indicators are frequently reported, subjective aspects, such as workload and perceived stress—critical for human-centered system design—are often underexplored.

This study investigated the reduction of human interference in HRC disassembly tasks. We developed a system that uses object detection to track the locations of humans, robots, and tasks. By evaluating different task types and algorithms, we provide empirical evidence of safety and efficiency trade-offs. The primary contribution of this study is an analysis of how task-algorithm pairings influence HRC workspace design to minimize human-robot conflict.

This study is organized as follows: Section II details the proposed HRC disassembly methodology and the technical architecture of the system design. Section III presents the experimental findings, followed by a discussion of the findings and limitations. Finally, Section IV concludes the study by summarizing the main contributions and future research directions.

II. Human-Robot Collaborative Disassembly

This section outlines the research methodology, including workspace setup and requirements, an overview of the system, applied algorithms, experimental design, and the evaluation using NASA-TLX. Fig. 1 presents an overview of the system, which tracks the real-time positions of the human, robot, and task locations. The architecture, based on an object detection algorithm, comprises two primary modules: a data processing unit for robot motion stimuli and a feedback determination component.

A. Workspace Setup

The experimental environment employed a DOBOT MG400, a lightweight industrial robot with a 30 cm $\times$ 20 cm workspace, selected for its high precision in intricate tasks. The AI-integrated camera served as a single sensor for real-time environmental mapping and object detection. In this collaborative disassembly scenario, human and robot worked in a shared workspace to perform sequential screw disassembly.

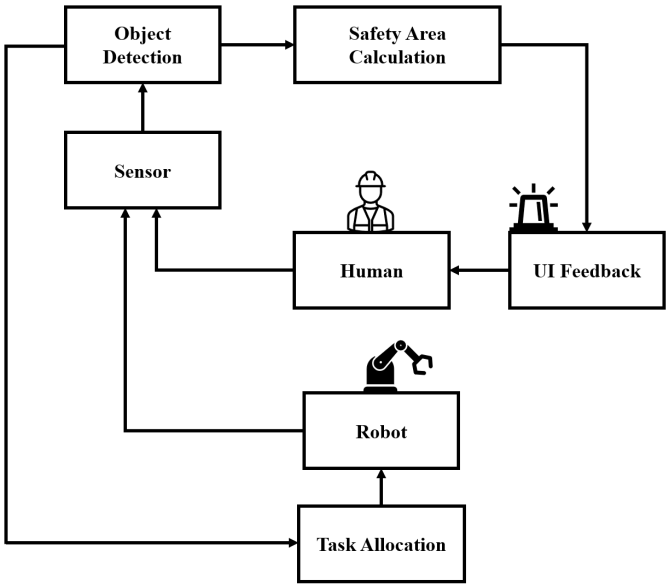

Fig. 1. Overview of proposed research.

To prioritize human safety, a task allocation algorithm dynamically adjusts the robot's target screw locations based on human movements. The experimental setup is shown in Fig. 2.

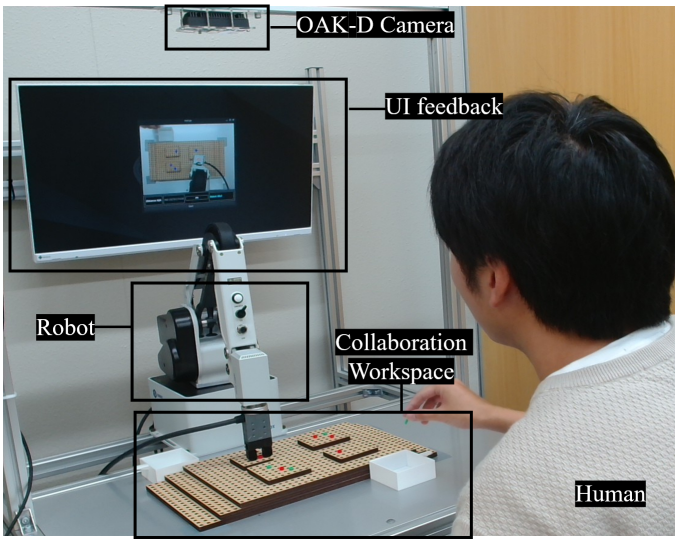

Fig. 2. Collaborative workspace setup.

The collaborative workspace was designed as a prototype for e-waste disassembly, using an MDF board for screw placement. Monitors integrated into the setup to provide real-time UI feedback, thereby facilitating communication between humans and robots. This UI displayed a safety zone, that was dynamically calculated via the human-robot object detection system to guide the user during the task.

B. Human-Robot Collaborative Algorithm

The proposed system uses object detection based on the YOLOv8 framework, selected for its proven real-time performance among state-of-the-art detection models. Detection accuracy and precision were evaluated through data collection, model training, and performance assessment.

The information obtained from the detected objects was in the form of x- and y-coordinates, with three labels. Assume that the coordinates of the humans, robots, and several screws are denoted as $H(x_h, y_h)$, $R(x_r, y_r)$, and $S_i(x_{si}, y_{si})$, respectively. This research focuses on the collaboration between a human hand and a robotic arm tasked with simultaneously picking up screws. In this study, distance calculations were required to measure the safety distance for collaboration. Eq. (1) was employed to obtain the real line distance from the x- and y-coordinates. This form is the absolute value between the human hand H and the screw S_i. where d_{HSi} is the distance between the hand and screw S_i. This distance was used for safety algorithm calculations. The calculation results serve as a stimulus for the robot to move toward the screw farthest from the human hand. Eq. (2) describes the calculation used to obtain the farthest distance. The detailed algorithm is described using the pseudocode Algorithm 1.

$$d_{HSi} = \|\mathbf{H} - \mathbf{S}_i\| \tag{1}$$

$$S_{far} = \max\{d_{HS1}(H, S_1), d_{HS2}(H, S_2), \ldots, d_{HSm}(H, S_m)\} \tag{2}$$

Algorithm 1 Safety Task Detection Algorithm

```
img ← cap_img()
H ← det_hand(img)
S ← det_screws(img)

for each S_i in S do
    dHS_i ← dist(H, S_i)
    if dHS_i > d_max then
        d_max ← dHS_i
        S_far ← S_i
    end if
end for
```

The human-robot distance, d_{HR}, is calculated using Eq. (3) and serves as a trigger for visual feedback.

$$d_{HR} = \|\mathbf{H} - \mathbf{R}\| \tag{3}$$

By observing the midpoint of both objects, safety considerations were divided into four areas calculated based on the distance between d_{min} 100 and d_{max} 400 pixels. These four areas indicate the level of danger, ranging from danger to caution, warning, and safety. Through distance normalization, as in Eq. (4):

$$\hat{d}_{HR} = min(\frac{d_{HR}}{d_{max}}, 1) \tag{4}$$

Denotes the normalized distance. This normalization maps the distance to a range of 0–1. If the human detection distance exceeded the d_{max} threshold, the person was automatically categorized as being in the safe zone. To visualize this on the

UI, the system calculates the inverse of the normalized distance to represent the danger level, as shown in the following Eq. (5):

$$D = (1 - \hat{d}_{HR}). \tag{5}$$

Eq. (6) defines four zones: danger, caution, warning, and safe. This zonal classification is fundamental to the HRC workspace, as it prioritizes collaborative safety.

$$f(D) = \begin{cases} \text{Danger}, & D > 0.5 \\ \text{Caution}, & 0.4 < D \leq 0.5 \\ \text{Warning}, & 0.3 < D \leq 0.4 \\ \text{Safe}, & D \leq 0.3 \end{cases} \tag{6}$$

This study investigated human responses to safety-based and random algorithms to assess their relative effectiveness. A combined approach integrating algorithm selection and UI feedback was implemented. Fig. 3 shows the UI feedback information used in this study, which includes the camera view serving as the sensing input, human-robot distance indicators for collision risk, and information on the screw selected for the robot pickup.

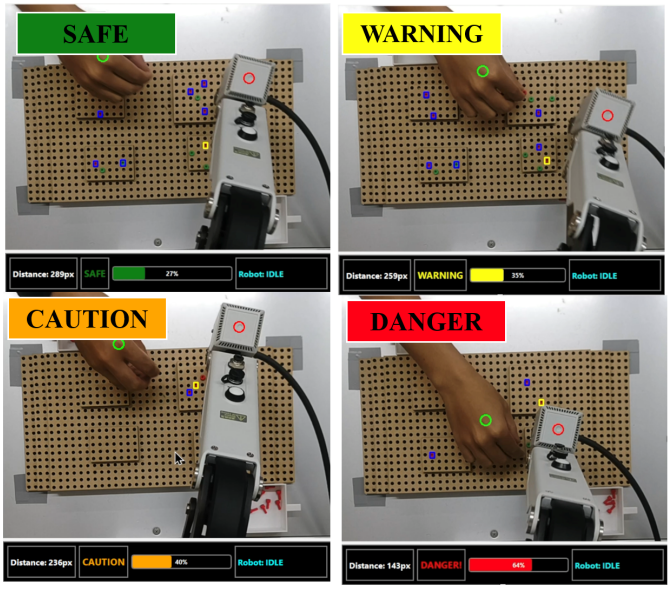

Fig. 3. Safety area UI feedback.

C. Experiment Design

The experiment involved five participants (aged 32 ± 8.3 years), each completing 10 trials per algorithm. Human responses to robot movements were evaluated using three objective parameters: task completion time, hand movement trajectories, and human-robot warning distance. Following the experimental trials, the participants completed a NASA-TLX questionnaire to assess perceived workload and system performance.

The algorithm was tested using two different task scenarios to obtain human behavior data. The separate target task (Task 1) involved 20 randomly positioned screws (10 red and 10 green screws). The robot retrieved the red screws until they were collected. The shared target task (Task 2) utilized 30 randomly positioned screws of the same color. The human-robot retrieved the screws until no screws remained. Fig. 4 illustrates the setup of Tasks 1 and 2.

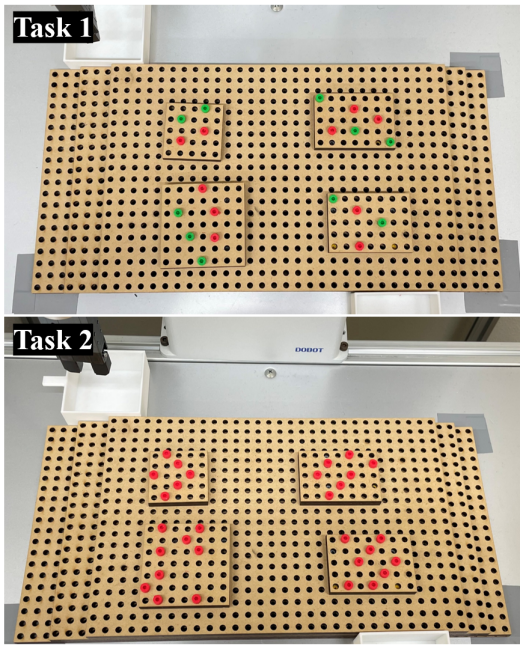

Fig. 4. Experiment task setup.

D. NASA-TLX Evaluation System

Subjective evaluation was conducted using the NASA-TLX questionnaire [13], which assess workload across six domains using a Likert scale: mental demand (MD), physical demand (PD), temporal demand (TD), performance (P), effort (E), and frustration level (FL). Participants completed the questionnaire after each experiment across the four distinct scenarios (comprising two tasks and two algorithms). The resulting data were analyzed using descriptive statistics to determine the impact of each scenario and identify significant differences in workload.

The use of NASA-TLX as a subjective evaluation identifies 'hidden costs' through direct participant feedback. Implementing such a human-centric system ensures that the operator's well-being is prioritized along with the robot's technical efficiency, providing a holistic justification for the system's deployment in industrial settings.

III. Experimental Results and Discussion

This section presents the experimental results and examines human behavior during collaborative disassembly tasks. The analysis focused on three key metrics: the completion time, frequency of proximity-based safety warnings (warning rate), and hand movements. The results of the NASA-TLX also captured the participants' perceptions.

A. Conditions

The participants were informed of the research objectives and experiments prior to providing informed consent, in accordance with the ethical requirements of the Saga University Ethics Committee (R4-38). During the experiment, the human and robot operated in a shared, barrier-free workspace, where collisions were possible. Fig. 5 shows the experimental setup in which the human and robot work together to retrieve screws until the workspace was cleared.

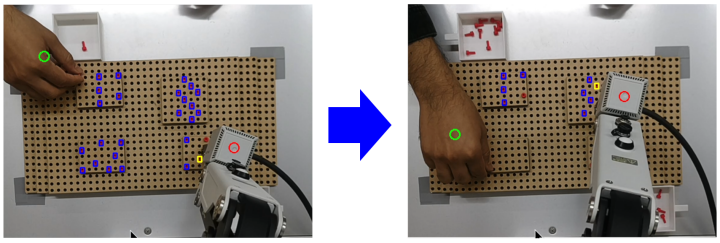

Fig. 5. Illustration of the retrieval process performed by the human-robot until task completion.

The experimental system was designed to facilitate data collection during human-robot collaboration. Following improvements in the object detection accuracy and real-time validation, the system was evaluated using both algorithms. Fig. 6 and Fig. 7 show the warning distance signals for the unconstrained and safe algorithms, respectively. The data show that the safety algorithm consistently maintains the required safety distance, confirming that the robot operates in accordance with the predefined safety thresholds.

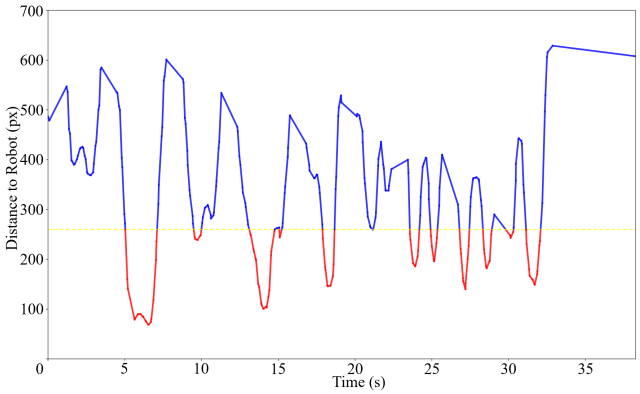

Fig. 6. Sample warning distance signals generated by unconstrained algorithm.

B. Results

The effects of algorithms and task types were examined using a factorial design, with statistical significance assessed via two-way ANOVA [14] at $\alpha < 0.05$. This analysis focused on the influence of these factors on completion time and total warning distance. Before the analysis, outliers were screened using the interquartile range (IQR) to ensure data integrity. Corresponding visualizations are presented in the bar charts in Fig. 8 and Fig. 9.

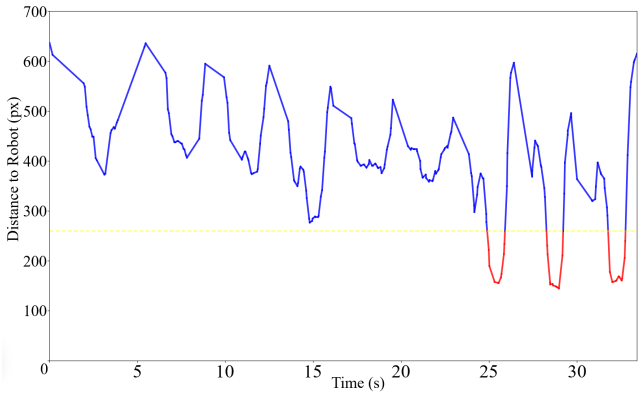

Fig. 7. Sample warning distance signals generated by safety algorithm.

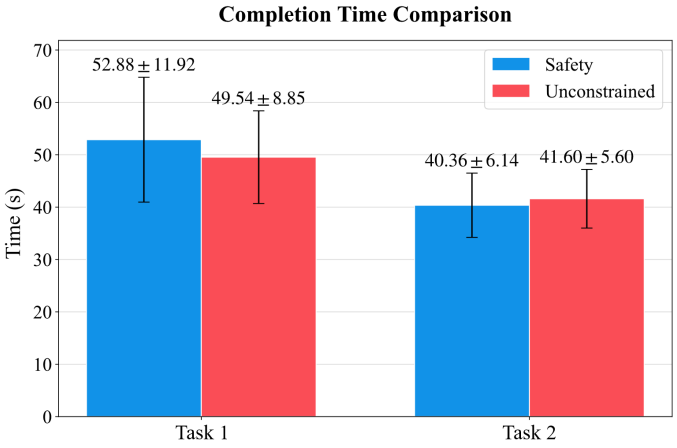

Fig. 8. Comparison of completion time performance for the safety and unconstrained algorithms during Task 1 and Task 2.

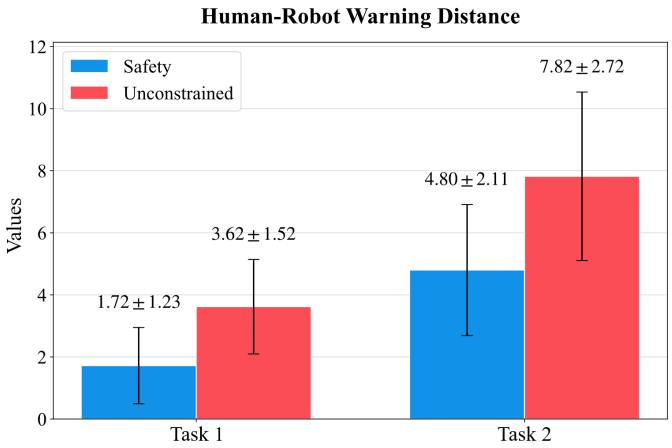

Fig. 9. Comparison of human-robot warning distance for the safety and unconstrained algorithms during Task 1 and Task 2.

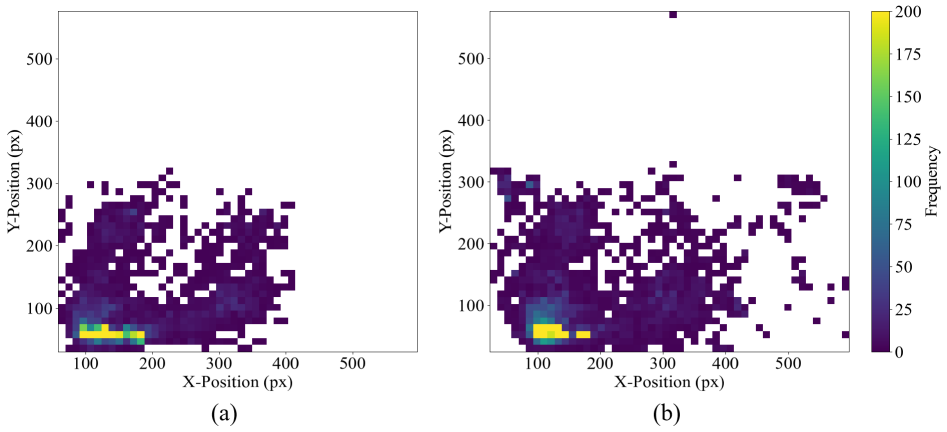

Fig. 10. Heatmaps of human hand movement during Task 1 for the (a) safety algorithm and (b) unconstrained algorithm.

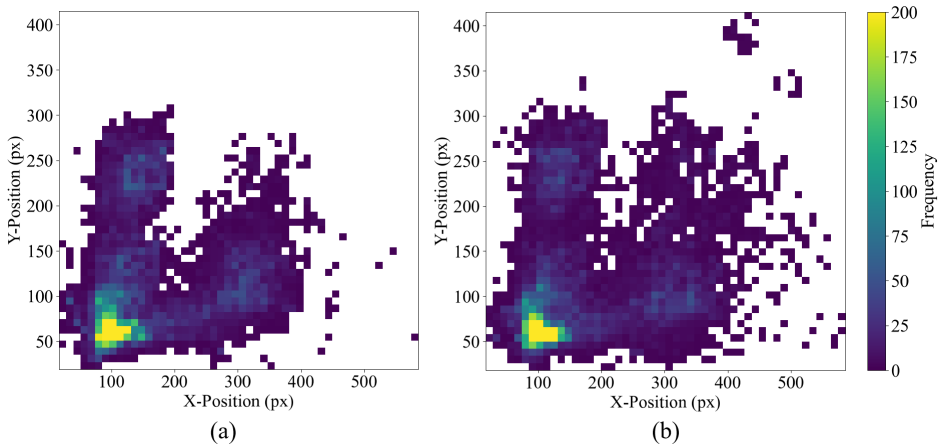

Fig. 11. Heatmaps of human hand movement during Task 2 for the (a) safety algorithm and (b) unconstrained algorithm.

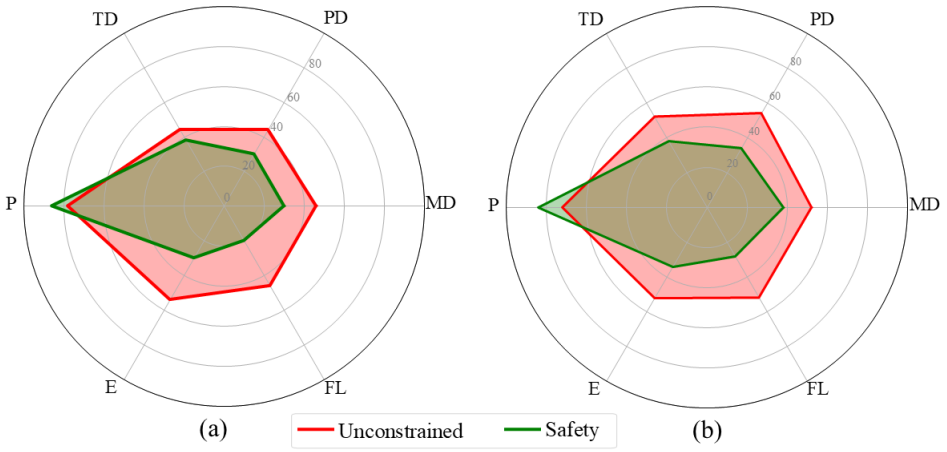

Fig. 12. NASA-TLX workload scores for (a) Task 1 and (b) Task 2 across both algorithms.

A two-way ANOVA conducted on completion time revealed a significant main effect for the task used ($F = 72.307$, $p < .001$, $\eta^2 = .269$). However, no significant main effect was found for the algorithm ($F = 0.76$, $p = .38$), and the interaction between algorithm and task did not reach statistical significance ($F = 3.62$, $p = .058$, $\eta^2 = .018$). These findings suggest that the differences in completion times were typically driven by the task itself, regardless of the algorithm being performed.

The two-way ANOVA for human-robot warning distance revealed significant main effects for both the algorithm ($F = 77.22$, $p < .001$, $\eta^2 = .283$) and the task ($F = 169.07$, $p < .001$, $\eta^2 = .463$). The interaction between algorithm and task was statistically significant ($F = 4.002$, $p = .047$, $\eta^2 = .02$). These results indicate that, while both the choice of algorithm and the specific task performed independently influenced the warning distance, the effect of the algorithm remained consistent across both tasks.

The spatial distribution of human movements was analyzed using heatmaps, as illustrated in Fig. 10 and Fig. 11 for Tasks 1 and 2, respectively. Comparative visual analysis revealed that the safety algorithm produced a significantly narrower distribution of human movement positions than the unconstrained algorithm. This concentration indicates that the safety algorithm facilitated a more predictable and structured human-robot interaction. These findings suggest that humans respond more effectively and consistently to robot movements when a safety algorithm is implemented.

Subjective assessments were performed using the NASA-TLX dimensions. A paired t-test confirmed a significant overall difference in Task 1 ($t = 4.402$, $p = .012$). In contrast to the previous measurements, the results for Task 2 were not statistically significant although they demonstrated a marginal trend ($t = 2.383$, $p = .076$). Fig. 12 shows the NASA-TLX differences between the two tasks.

C. Discussion

Experimental results indicate that the proposed algorithm significantly modulates human behavior during robot collaboration. Although real-time human movement remains unpredictable, spatial mapping using heatmaps reveals distinct behavioral patterns. Specifically, human responses were more efficient and localized when collaborating with a safety-constrained robot, indicating predictable robot movements and an enhanced sense of human safety.

Despite identical workspace dimensions, task type significantly influenced movement distribution. In Task 1 (a Separate Task), the range of human movement was much narrower than that in Task 2 (a Shared Task). This difference in spatial distribution is corroborated by the human-robot warning distance data, suggesting a lower collision probability for Task 1. This finding suggests that the separate task facilitates a safer environment by allowing humans to anticipate robot trajectories more effectively, whereas the shared task requires a wider range of avoidance maneuvers, and thus, is more complex. The integration of task assignment with safety algorithms yields results that minimize human interference.

D. Limitations

A collaborative disassembly system was developed to address the primary research questions. However, further investigation is needed to assess the system's long-term sustainability and robustness. Considering the limited sample size, the current findings may have restricted generalizability. Broader validation with a larger and more diverse population is required to support public and industrial adoption.

In addition, current hardware configurations would benefit from sensor redundancy. Although the vision-based approach effectively preserves human flexibility during collaboration, the camera's limited field of view necessitates additional sensors to mitigate occlusion issues.

IV. Conclusion and Future Work

This study investigated human interference during collaborative disassembly. The proposed safety algorithm significantly reduced the frequency of hazard warnings. Furthermore, NASA-TLX evaluations indicated that distinct task allocation, combined with feedback information, facilitated better maintenance of human-robot separation distances compared to shared-task execution. These results suggest that humans anticipate robot trajectories when task objectives are clearly defined in advance.

Note that the current disassembly process is a prototype involving simplified tasks. Future work will focus on optimizing the safety algorithm to prevent collisions during the final few tasks, thereby enhancing both efficiency and ergonomic outcomes. Additional studies with larger and more diverse participant groups are needed to improve the scalability of industrial applications.

Acknowledgment

This study was funded by JSPS KAKENHI (grant number 23H03440).

References

[1] M. Dhanda, B. A. Rogers, S. Hall, E. Dekoninck, and V. Dhokia, "Reviewing human-robot collaboration in manufacturing: Opportunities and challenges in the context of industry 5.0," *Robotics and Computer-Integrated Manufacturing*, vol. 93, p. 102937, Jun. 2025. [Online]. Available: https://linkinghub.elsevier.com/retrieve/pii/S0736584524002242

[2] S. Proia, R. Carli, G. Cavone, and M. Dotoli, "Control Techniques for Safe, Ergonomic, and Efficient Human-Robot Collaboration in the Digital Industry: A Survey," *IEEE Transactions on Automation Science and Engineering*, vol. 19, no. 3, pp. 1798–1819, Jul. 2022. [Online]. Available: https://ieeexplore.ieee.org/document/9638383/

[3] K. Liu, Q. Tan, J. Yu, and M. Wang, "A global perspective on e-waste recycling," *Circular Economy*, vol. 2, no. 1, p. 100028, 2023.

[4] R. Ahirwar and A. K. Tripathi, "E-waste management: A review of recycling process, environmental and occupational health hazards, and potential solutions," *Environmental Nanotechnology, Monitoring & Management*, vol. 15, p. 100409, 2021.

[5] A. Morachioli, V. Sivtsov, N. Rojas, and F. Bonsignorio, "A Functional and Practical Taxonomy for the Industrial Implementation of Highly Automated Reverse Manufacturing Cells," *IEEE Open Journal of the Industrial Electronics Society*, vol. 5, pp. 1115–1139, 2024. [Online]. Available: https://ieeexplore.ieee.org/document/10666886/

[6] M. Caterino, M. Rinaldi, V. Di Pasquale, M. Fera, and D. T. Pham, "Addressing the impact of robots during disassembly operations: results from an empirical study," *International Journal on Interactive Design and Manufacturing (IJIDeM)*, Aug. 2025. [Online]. Available: https://link.springer.com/10.1007/s12008-025-02383-7

[7] J. Huang, D. T. Pham, R. Li, M. Qu, Y. Wang, M. Kerin, S. Su, C. Ji, O. Mahomed, R. Khalil, D. Stockton, W. Xu, Q. Liu, and Z. Zhou, "An experimental human-robot collaborative disassembly cell," *Computers & Industrial Engineering*, vol. 155, p. 107189, May 2021. [Online]. Available: https://linkinghub.elsevier.com/retrieve/pii/S0360835221000930

[8] F. Barravecchia, M. Bartolomei, L. Mastrogiacomo, and F. Franceschini, "Designing Symbiotic Human–Robot Collaboration in assembly tasks," *Production Engineering*, vol. 19, no. 3-4, pp. 629–661, Jun. 2025. [Online]. Available: https://link.springer.com/10.1007/s11740-025-01333-2

[9] W. Xu, Q. Tang, J. Liu, Z. Liu, Z. Zhou, and D. T. Pham, "Disassembly sequence planning using discrete Bees algorithm for human-robot collaboration in remanufacturing," *Robotics and Computer-Integrated Manufacturing*, vol. 62, p. 101860, Apr. 2020. [Online]. Available: https://linkinghub.elsevier.com/retrieve/pii/S0736584519301887

[10] S. Parsa and M. Saadat, "Human-robot collaboration disassembly planning for end-of-life product disassembly process," *Robotics and Computer-Integrated Manufacturing*, vol. 71, p. 102170, Oct. 2021. [Online]. Available: https://linkinghub.elsevier.com/retrieve/pii/S0736584521000545

[11] M.-L. Lee, S. Behdad, X. Liang, and M. Zheng, "Task allocation and planning for product disassembly with human–robot collaboration," *Robotics and Computer-Integrated Manufacturing*, vol. 76, p. 102306, Aug. 2022. [Online]. Available: https://linkinghub.elsevier.com/retrieve/pii/S0736584521001861

[12] M.-L. Lee, W. Liu, S. Behdad, X. Liang, and M. Zheng, "Robot-Assisted Disassembly Sequence Planning With Real-Time Human Motion Prediction," *IEEE Transactions on Systems, Man, and Cybernetics: Systems*, vol. 53, no. 1, pp. 438–450, Jan. 2023. [Online]. Available: https://ieeexplore.ieee.org/document/9817380/

[13] A. K. Eesee, V. Varga, G. Eigner, and T. Ruppert, "Impact of work instruction difficulty on cognitive load and operational efficiency," *Scientific Reports*, vol. 15, no. 1, p. 11028, Apr. 2025. [Online]. Available: https://www.nature.com/articles/s41598-025-95942-7

[14] C. Andrade, "Understanding Factorial Designs, Main Effects, and Interaction Effects: Simply Explained with a Worked Example," *Indian Journal of Psychological Medicine*, vol. 46, no. 2, pp. 175–177, Mar. 2024. [Online]. Available: https://journals.sagepub.com/doi/10.1177/02537176241237066